Journal of Flood Risk Management

WILEY

CIWEM Chartered Institution of Water and Environmental Management | Journal of Flood Risk Management

SPECIAL ISSUE PAPER OPEN ACCESS

Integration of Stability Functions Into a Transport Flood Risk Modelling Framework

Lea Dasallas | Barry Evans | Dion Todd | Hamish Kampman | Markus Pahlow | Thomas A. Cochrane

Department of Civil and Environmental Engineering, University of Canterbury, Christchurch, New Zealand

Correspondence: Barry Evans (barry.evans@canterbury.ac.nz)

Received: 28 January 2025 | **Revised:** 8 October 2025 | **Accepted:** 28 October 2025

Funding: This work was supported by the European Union's Horizon Europe Framework Programme for Innovation under grant agreement (101147385).

Keywords: accessibility modelling | stability function | transport flood risk analysis | urban flooding

ABSTRACT

The increasing frequency of urban flooding due to climate-induced extreme rainfall highlights the critical need for adaptive emergency preparedness. Maintaining public access to essential services during such events is critical, yet flood risks to the transport network can compromise public safety and mobility. This study employed a combined depth-velocity stability function to assess the risks posed to individuals navigating floodwaters and evaluates accessibility to key service points using basic risk-avoidance criterion. Transport network analysis compares the no-flood, depth-only and depth-velocity risk scenarios. Analysis indicates that risk assessments solely based on flood depth significantly underestimate localised risk in urban environments. At the flood peak, high-risk areas for vehicles and pedestrians are underestimated by 18.2% and 83.3%, respectively, while these increase to 36.4% and 240.0% for medium-risk areas. Applying depth-velocity thresholds determined the obstructed roads and inaccessible zones. Risk-adjusted alternative routes were generated considering the obstructions, providing viable paths for the public to use during the flood peak. The integrated approach, combining flood modelling, stability functions and network analysis offers a framework that can significantly contribute to the improvement of risk resilience and transport management for flood-prone cities.

1 | Introduction

Changes in intensity and duration of extreme rainfall events in New Zealand and around the world have resulted in a greater number of events exceeding the design capacities of current stormwater infrastructure (Bisht et al. 2016; Hettiarachchi et al. 2018; Le et al. 2024). The information obtained from flood models is crucial in developing viable solutions by modelling required additional or improved urban flood mitigation infrastructure, or planning emergency evacuation to minimise the negative impact of flooding (Pants et al. 2018). Oftentimes, priorities shift the focus from infrastructure solutions to the need for improving emergency management planning, such as developing flood evacuation routes or access to emergency services (Harris et al. 2021). Effective flood planning is not only proven to minimise losses but also reduces the recovery time for the population affected by the flood event (Petrucci et al. 2017).

One of the key safety issues encountered during flood events is the potential risk in transiting through the transport network using vehicles or by foot (Pregnolato et al. 2017). As the stormwater network becomes overwhelmed, the transport network then acts as the path for concentrated overland flow (Hsu et al. 2000; Paquier et al. 2015). These hazards necessitate the enforcement of emergency response measures, including mobilisation of specialised services, and the initiation of protocols to ensure public safety during the event. Planning transport mobility should carefully consider the road networks that are at risk of road surcharges during flood events. Such considerations are specifically critical for areas where the local topography is

characterised by steep slopes and narrow passages, since these parts of the transport network can serve as the 'bottleneck' sites for flood flows (Flores et al. 2024).

Quantifying the associated flood threats in the transport network is therefore necessary in order to effectively mitigate the potential mobility risks during flood events. A conventional approach in assessing the accessibility of the transport network mainly relies on quantifying the flood risk based exclusively on flood depth. This method only applies an inundation depth threshold to evaluate the impact of flooding on the accessibility and mobility of pedestrians and vehicles within the transport network. Recent studies focusing on this concept include the analysis of the accessibility of transport routes based on flood depth in dense urban areas (Yang et al. 2023), modelling of evacuation routes based on single vehicle-class flood depth and shortest travel time (Melo et al. 2014) and analysis of routes based on pedestrian movement time in response to flood depth (Lee et al. 2024). These approaches, however, did not incorporate the velocity component of the flood water, which had been found to significantly pose a risk to the safety of transit users.

The inclusion of the flood-velocity component in planning is especially important for urban catchments with steep and impervious surfaces, where the runoff velocity is often intensified. Incorporating flood flow velocity is identified as one of the key factors in structural damage and casualties; considering both flood depth and velocity provides a more accurate representation of expected urban flood damage (Adeke and Mugume 2025). Such conditions can strongly affect the stability of both pedestrians and vehicles (Falconer et al. 2015). Quantifying the pedestrian and vehicle flood risk can be more appropriately approximated using a flood depth-velocity stability function (Pregnolato et al. 2017). This approach can be complex, as the risk approximation is dependent on the features of the person or vehicle being modelled. To establish a unified standard and simplify the estimations, a maximum depth-velocity criterion is developed in the Australian Rainfall and Runoff guidelines, obtained through people and vehicle stability experiments (Cox et al. 2011). The depth-velocity functions were further improved in the theoretical and experimental studies performed for pedestrians (Martínez-Gomariz et al. 2016) and vehicle stability (Martínez-Gomariz et al. 2017), identifying that stability is significantly influenced by human factors such as weight, height or posture, and hydrodynamic forces such as drag, rolling resistance and buoyancy for vehicles. These studies highlight the potential of using established depth-velocity thresholds to identify safe transport routes and maintain network accessibility under flood risk conditions. However, research on transport network analysis for network mobility focusing on the accessibility of transport routes that utilise both depth and velocity stability functions for urban flood events remains highly limited. While studies have emphasised the importance of incorporating both flood depth and velocity into a more accurate representation of damage estimates, a quantifiable comparison of these approaches, one based on flood depth alone and the other on both flood depth and velocity, is yet to be explored specifically within the context of transport network accessibility. For instance, research by Adeke and Mugume (2025) highlighted the need for more accurate flood depth-velocity damage functions, while He et al. (2024) evaluated the effect of integrated flood hazards on road functionality and accessibility. Similarly, Pregnolato et al. (2017) established a relationship between flood depth and vehicle speed in the transport network while Evans et al. (2023) assessed the risk posed to individuals and vehicle occupants by analysing the scenarios to determine their safety while waiting for help or exiting. However, the broader issue of transport network accessibility and emergency management during large-scale urban flood events imposes a more realistic problem to solve. Identifying the areas in the transport network that are also at risk based on the velocity of the flood flow is integral to the safety of the public in the case of flood events. To close this research gap, the aim of the current work is to develop a framework that quantifies the at-risk areas in a transport network including stability functions that consider flood depth only and both flood depth and velocity for an urban environment with a range of topography.

The specific research objectives are to (1) model the 1D–2D flow interaction of selected urban sub-catchments, (2) develop flood risk maps that account for both depth, and depth-velocity stability functions, (3) conduct transport network analyses for critical facilities and key sites for the urban population under dry conditions, flood depth-only risk and flood depth-velocity risk network obstruction conditions, and lastly, (4) provide a methodology framework that can be used to improve transport mobility management for cities and flood event emergency response approaches with mixed steep and flat urban catchments. We propose a management method that could be used to enhance urban resilience to flooding, adapting planning solutions for future climate challenges.

2 | Methods and Data

2.1 | Methods

The overall modelling framework, shown in Figure 1, incorporates the 1D/2D flood models that output spatial data comprised of flood depth and flow velocity at regular time intervals. Through utilising depth-only and depth-velocity stability curves for vehicles and pedestrians, these outputs are translated into risk maps, that are then overlaid onto the transportation network. Using urban mobility for route analysis and pre-defined origin–destination data, the accessibility of the transport network is assessed at regular time intervals for both vehicles and pedestrians, whereby they are not allowed to traverse sections deemed to be at risk during the modelled time interval.

2.1.1 | Urban Flood Simulation

PC Storm Water Management Model (PCSWMM Version 7.6.3695), developed by Computational Hydraulics Inc. (CHI), was used to simulate urban flooding (Computational Hydraulic Inc. 2025). PCSWMM is a globally utilised flood model that has the capability to simulate surface and sub-surface flow interactions and has been a proven effective tool for urban flood analysis (Sidek et al. 2021). The surface runoff in PCSWMM is calculated when the water depth in the sub-catchment surface 'reservoir' exceeds the maximum depression storage (EPA 2015). The flow velocity is calculated using the Manning equation on

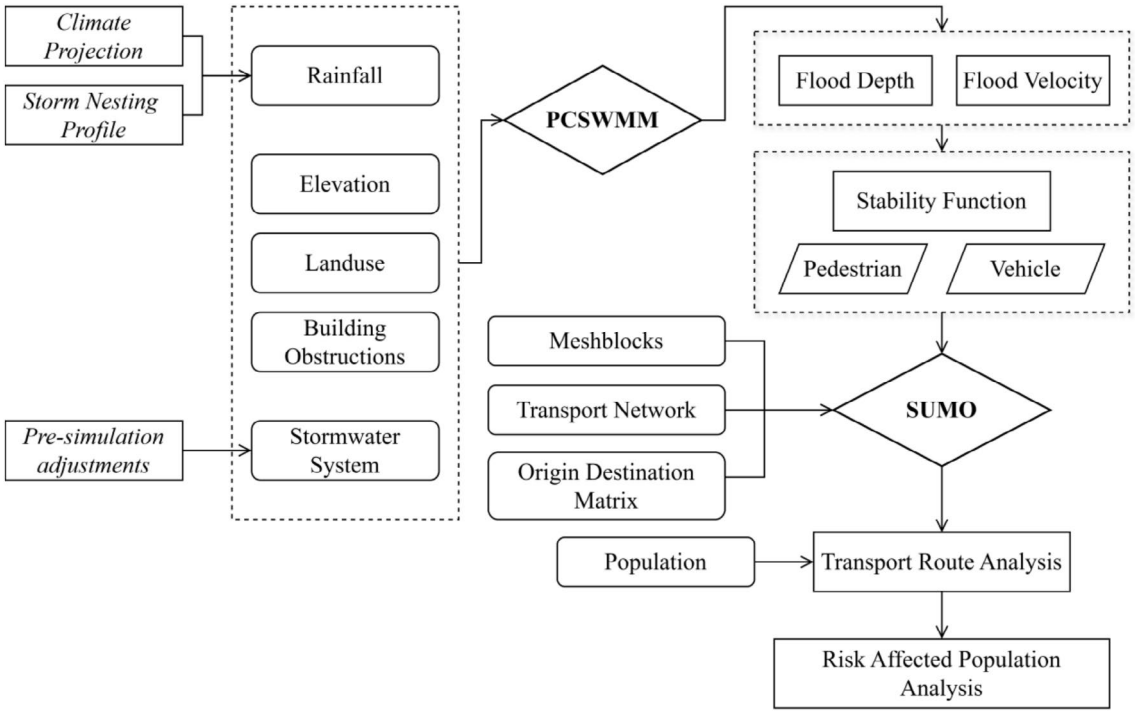

FIGURE 1 | Methodology schematic diagram discussing flood model input parameters, flood model simulation using PCSWMM, vehicle and pedestrian stability function risk calculation, transport network analysis using SUMO and analysis of risk-affected population.

open channel flow based on channel characteristics, slope and roughness.

$$V = \frac{1}{n} R^{2/3} S^{1/2} \quad (1)$$

where the velocity is dependent on the flood depth approximation in shallow water (R), surface roughness coefficient (n) and slope of the surface (S).

In recent years, PCSWMM has been widely used and calibrated for various hydrological and hydraulic applications, including inflow and runoff (Ahiablame and Shakya 2016; Randall et al. 2017; Zhang and Valeo 2022), flood depth and extent (Bibi et al. 2023; Du et al. 2025; Manchikatla and Umamahesh 2022; Sidek et al. 2021) and flow velocity assessments (de Castro-Ferreira et al. 2022; Sangal and Bonema 1994). Calibration results have generally demonstrated satisfactory performance. For instance, Sidek et al. (2021) reported an R-squared value of 0.68 for water depth calibration, while Randall et al. (2017) achieved Nash–Sutcliffe efficiency (NSE) values of 0.86 and 0.82 for maximum and total flow, respectively, demonstrating the model's reliability and suitability for diverse modelling scenarios.

To represent the stormwater drainage network and overland flow, 1D–2D models for the study area sub-catchments were developed. 2D surface runoff modelling requires digital elevation model (DEM), catchment boundary, building outlines and rainfall hyetograph data. A multi-resolution hexagonal mesh was set up to represent road and building area (6 m resolution), combined urban and green areas (14 m) and green spaces (24 m) to optimise the flood accuracy and computation time. The surface roughness coefficient was set as $0.016\,s/m^{1/3}$ for roads, buildings and parking space, $0.025\,s/m^{1/3}$ for residential areas and parks and $0.070\,s/m^{1/3}$ for forests and vegetation, respectively (Wellington Water 2021). The flood cells, stormwater network, building obstructions and the different surface type cell resolutions are shown for a sub-section of the study catchment in Figure 2. Building obstructions represent buildings and artificial structures that can hinder, restrict and/or redirect flood flow.

To represent a worst-case scenario for flooding, the antecedent soil conditions, infiltration, evaporation and evapotranspiration processes are not incorporated in the simulations. The evaporation and evapotranspiration parameters are omitted as their effects for individual storm events are relatively negligible with respect to the timescale and usually not included to simplify computations (Haan et al. 1994). The exclusion of the infiltration process, on the other hand, adheres to an assumption that the soil is already saturated and unable to absorb additional floodwater, leading to maximum potential runoff. During periods of high rainfall intensity, surface runoff becomes the dominant component of total runoff, especially under conditions of high antecedent wetness when parts of the catchment are already saturated (Bronstert et al. 2022). This would represent a worst-case scenario flooding, for instance, where there were (1) precedent storm or monsoonal rains and (2) the majority of the urban surface is composed of impermeable materials. This assumption was also considered with the highest level of rainfall extreme utilising an extreme return period and a climate projection associated with the highest greenhouse gas emissions, thereby theoretically representing severe consequences in precipitation extremes.

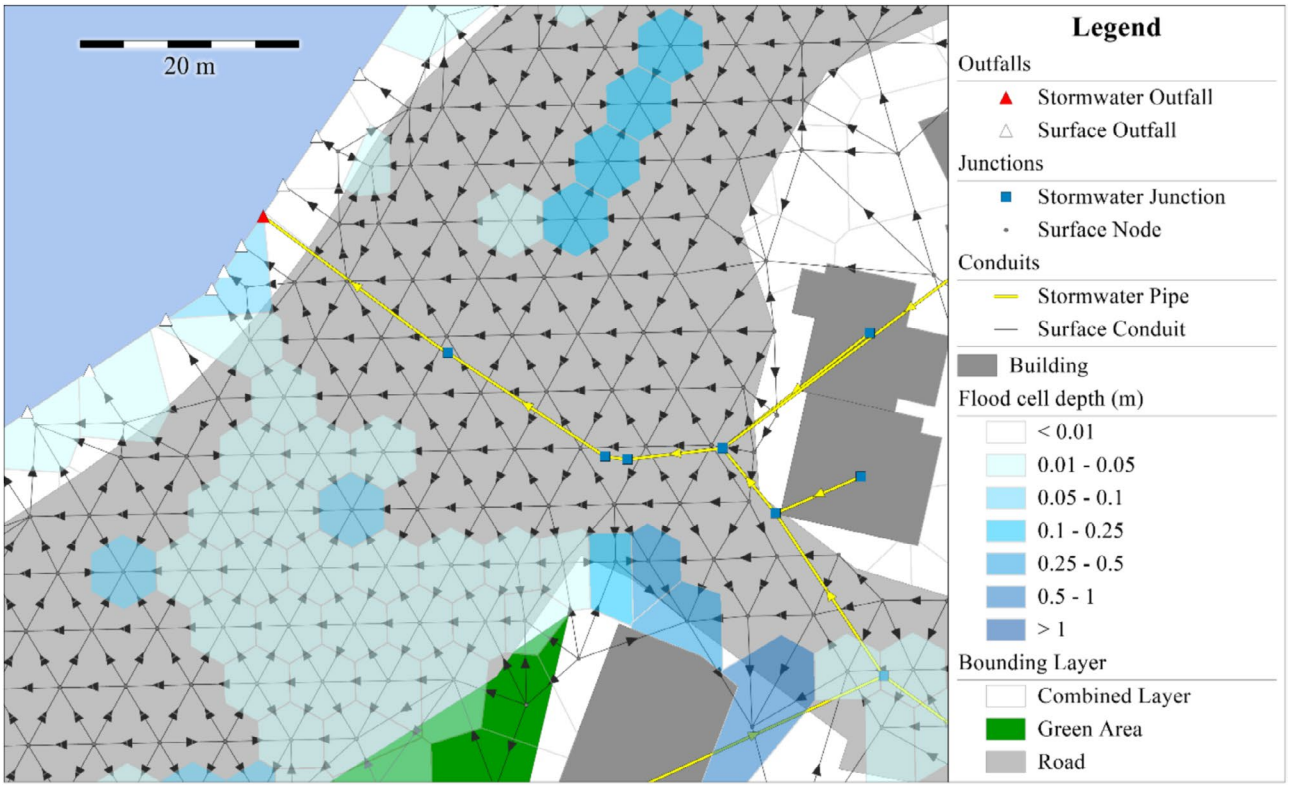

FIGURE 2 | 2D surface grids and 1D stormwater network for a sub-section of the study area.

For cases where data were missing, assumptions were made to complete the model set up, as detailed in Table 1. Limitations in the availability of comprehensive stormwater networks have posed challenges in simulating urban flooding in recent years (Bertsch et al. 2017; Jeffers and Montalto 2018). Some solutions include simplifying the network by making assumptions based on field surveys, proximity and extrapolation using spatial analysis methods. For this research, the assumptions are derived from literature, or the average values of the surrounding units were used. These assumptions include connecting isolated sumps to the network if they are within a road distance from the nearest network sump, missing pipe diameter data matching the surrounding pipe values, or missing pipe material data assumed to be the most common pipe material in the study area.

2.1.2 | Stability Function for Risk Assessment

Depth and velocity stability functions determine the stability of the pedestrians and vehicle occupants during evacuation (Cox et al. 2011). Stability thresholds are defined as the value of the flood flow depth and velocity that pose potential risks for pedestrians or vehicles to be overwhelmed or swept away. These risks can cause physical or property damage, or potentially loss of life (Evans et al. 2023). The stability functions overlaid with the depth-only and depth-velocity criteria, showing the different risk thresholds for pedestrians and vehicles are displayed in Figure 3. High Risk Depth-Only and Depth-Velocity (HRDO and HRDV) refer to the depth and depth-velocity threshold risks for everyone including adults under normal conditions and large passenger vehicles. Conversely, Medium Risk Depth-Only and Depth-Velocity (MRDO and MRDV) pertain to the depth and depth-velocity threshold risks for children, the elderly, and small passenger vehicles.

The stability thresholds are derived from experimental studies that determined critical flow stability limits for pedestrians to be swept away (Martínez-Gomariz et al. 2016) and vehicles becoming buoyant (Martínez-Gomariz et al. 2017). The pedestrian stability experiment analysed flood depth and velocity to determine the conditions that can trigger sliding and toppling, leading to pedestrian instability. The toppling phenomenon occurs when the oncoming flow force exceeds stability based on body weight, while sliding happens when the horizontal flow drag force becomes greater than the frictional resistance between the person and the ground surface. In addition to sliding and toppling, vehicle instability also leads to floating failures, which occur when the flood depth is high enough to subject the partially submerged vehicle to buoyancy force. When this occurs, vehicles can be swept away colliding with urban elements, which could result in significant injuries or fatalities, potentially compromising the safety of transport users.

For this research, the values of flood depth and velocity are calculated for each timestep. For the depth-only risk analysis, a flood cell is considered high risk if the flood depth exceeds the depth thresholds, regardless of the value of flood velocity. For the depth-velocity risk analysis, however, only the flood cells that exceeded the combined depth-velocity threshold, are considered. The timestep with the greatest number of high-risk flood cells over the study domain, which also equates to

the timestep with the greatest number of high-risk cells coinciding with the road network, represents the flood risk maps. This method ensures that the worst-case scenario flood is represented in the highest-risk scenario in modelling the extreme flood events.

TABLE 1 | Key assumptions implemented for the preparation of the stormwater data.

If data were missing	Assumption
Pipe diameter	Assumed to be the same diameter as the centroid of the nearest pipe with known diameter
Inlet	Upstream network pipes without connecting sumps are assumed to have a sump at the upstream point
Crown level	The crowns of the pipes are assumed to have a network average of 1.5 m below ground level
Sump connection	Isolated sumps are connected to the network if the sumps are within 15 m (average road width) of the nearest stormwater node. Otherwise, the isolated sump is deleted
Sump geometries	Assumed to be a standard single grate sump specified by Wellington Water (2021)
Pipe materials/ Manning's coefficient	Assumed to be the most common WCC pipe material (concrete and cast iron) with a Manning's n value of 0.012 s/m$^{1/3}$
Building connections	Building nodes are generated to connect the rainfall accumulation in the buildings directly to the stormwater network

2.1.3 | Transport Network Risk Analysis

For the transport risk analysis, the key destination point data, road network and population data are analysed using the Simulation of Urban MObility (SUMO) software. SUMO is an open-source platform that performs microscale transport simulations, capable of considering time-discrete and space-continuous traffic flow for both pedestrians and vehicles (Eclipse SUMO 2025). SUMO has been increasingly adopted in recent literature to simulate traffic dynamics under various hazard scenarios, including flood-impacted traffic flow (Evans et al. 2020), wildfire evacuation (Filippidis et al. 2020) and tsunami evacuation scenarios (Fathianpour et al. 2023). Its application in traffic mobility modelling has been validated through numerous studies (Chowdhury and Chakraborty 2024; Ivanov and Abu-Abed 2019; Rahman et al. 2019), Fathianpour et al. (2023) validated SUMO travel time and total number of successful evacuations against real-life tsunami evacuation drills. Chowdhury and Chakraborty (2024) performed calibrations of SUMO queue and travel time based on observed traffic patterns to accurately replicate cities with diverse traffic conditions. Similarly, Ma et al. (2021) verified the traffic conditions generated from SUMO using real traffic data. These studies demonstrated SUMO's reliability and suitability for dynamic transport simulation under normal and hazard-induced conditions. SUMO can employ Dijkstra's or A* path-finding algorithms to determine the shortest and/or fastest route from a starting point to a destination point. Here, the default Dijkstra's algorithm was applied to define routes from origins to destinations.

To define the start location/origins for these simulations, we have utilised 'meshblocks', the smallest geographic units used for representing statistical data in New Zealand. The origin–destination matrices were defined such that each road or sidewalk segment within a meshblock can be considered as an

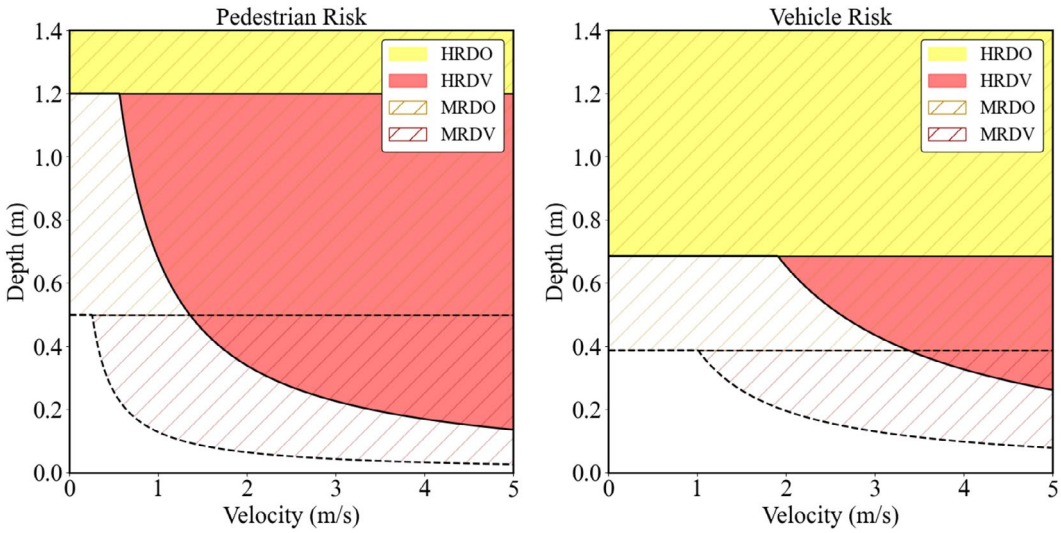

FIGURE 3 | Medium and high depth-only and depth-velocity risks for pedestrians (Martínez-Gomariz et al. 2016) and vehicles (Martínez-Gomariz et al. 2017).

TABLE 2 | Input data used for the Wellington sub-catchments study.

Input data	Description	Data source
Climate projected rainfall data	HIRDS Depth-Duration-Frequency Rainfall	National Institute of Water and Atmospheric Research (2024b)
Digital elevation model (DEM)	Wellington City LiDAR 1 m DEM (2019–2020)	Land Information New Zealand (2024)
Catchment outline	Lambton/Northern CBD Catchment (2022)	Wellington City Council (2024)
Land use data	Wellington City Council (WCC) Land Use	Wellington City Council (2024)
Building outlines	NZ Building Outlines (2024)	Land Information New Zealand (2024)
Stormwater pipe network data	WCC 3Waters Asset Data	Wellington City Council (2024)
Transport network data	Open Street Map Data	OpenStreetMap Contributors (2025)
Meshblocks data	Meshblock Statistical Data	Stats New Zealand (2024)
Population data	2018 Census Electoral Population	Stats New Zealand (2024)

origin start point, while the assigned key destinations, such as essential transport services and facilities, are considered as the potential destination points. Flood risk analysis, utilising depth-only and depth and velocity stability functions, is performed to determine which roads and sidewalks are blocked to vehicles and pedestrians at each 1-h time interval. Using an iterative approach, routing analysis is carried out for each time interval (for pedestrians and vehicles separately), from each starting meshblock to the destination points. If at least one origin–destination pair resulted in a valid route, the meshblock was classified as maintaining accessibility to its designated point; whereby, if no valid routes could be found, the meshblock was considered inaccessible for that time interval for the given mode of transport. By utilising this approach, a comprehensive comparison of how transport accessibility can change during an event can be carried out. This method enables detailed analysis on the influence of flow velocity on transport accessibility and mobility into risk assessment frameworks.

2.2 | Data

The model input data used to simulate the urban flooding for the study area, descriptions and their corresponding data sources, are summarised in Table 2. The flood model input includes rainfall, elevation, land use, catchment boundary, building obstruction and stormwater network. Transport risk modelling requires data on the road network, meshblocks, population and the location of the key destination points.

Extreme rainfall events in New Zealand are defined as rainfall exceeding 100 mm in 24 h (National Institute of Water and Atmospheric Research 2024a). To represent the worst-case flooding scenario for this research, the climate projected RCP 8.5 (Representative Concentration Pathway) rainfall intensity data from the NIWA-developed High Intensity Rainfall Design System (HIRDS) V4 was utilised (NIWA 2018). The RCP 8.5 climate scenario represents the highest risk, characterised by continuous rise and acceleration of greenhouse gas concentrations compared to the current state. For this research, a synthetic 24 h 250-year average recurrence interval (ARI) climate projected nested rainfall hyetograph was used in the simulations, shown in Figure 4. The peak was set at the second tercile, specific to the case study, as suggested from the Wellington Water Reference Guide for Design Storm Hydrology (Wellington Water 2019).

High-resolution DEM (1 m) data were obtained from LiDAR (Light Detection and Ranging) aerial survey, and the building obstruction outline data were provided by Land Information New Zealand (LINZ). The sub-catchment outlines used to set the model boundary, the land use data used to establish the surface roughness values, and the stormwater pipe network data for the sub-surface simulation are obtained from the Wellington City Council (WCC). The population information was gathered from the 2018 Census Electoral Population data. For the transportation network, OpenStreetMap data for the Wellington region was obtained and converted utilising SUMO's 'netconvert' tool (Lopez et al. 2018) for use within the SUMO traffic model along with the option of adding sidewalks to road sections for pedestrian modelling scenarios (OpenStreetMap Contributors 2025).

2.3 | Case Study Area

The catchment selected for the development and application of the framework is the Lambton and Northern Central Business District (CBD) catchment in Wellington, New Zealand. The catchment has a total area of 13.67 km^2 and contains three smaller sub-catchments, namely Oriental Bay and Northern and Southern CBD (Figure 5). The urban sub-catchments were selected due to their mixed steep and flat topography characteristics, a combination of hilly and coastal impervious surfaces that make the densely populated area susceptible to flood risks. The transport network, meshblock zones and location of the assigned destination points are also shown in Figure 5.

A considerable section of the catchment area is identified as low-lying reclaimed land. These areas are heavily developed and contain the key transport network for the central business district (Wellington City Council 2024). Factors such as the complex topography and bottleneck transport network routes can present challenges in the development of emergency management strategies for central Wellington. These challenges emphasise the importance of having an in-depth understanding of

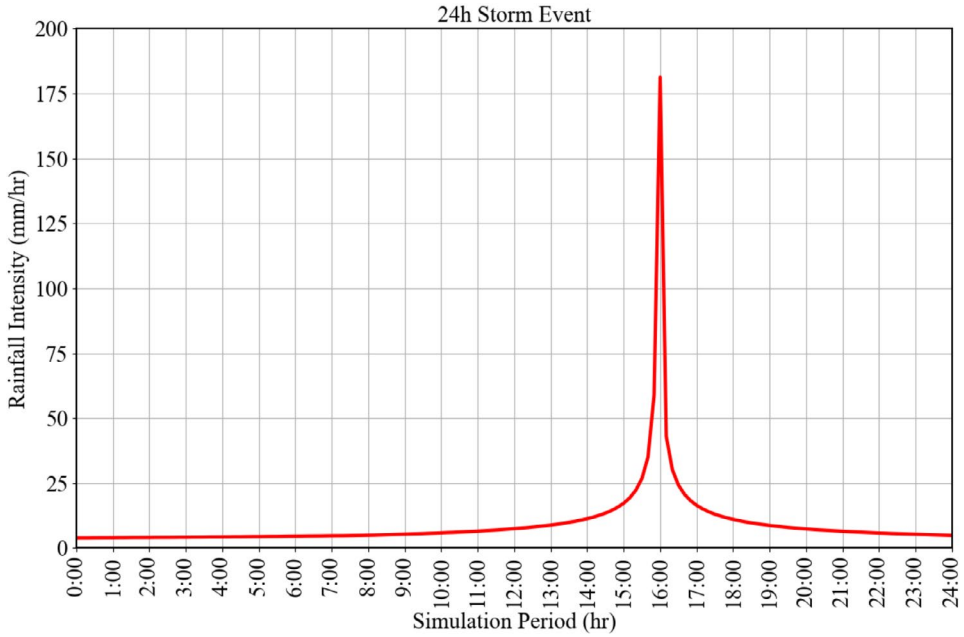

FIGURE 4 | Synthetic 24-h nested storm profiles based on 250-year RCP 8.5 climate projected rainfall intensities.

the risk and transport accessibility to critical infrastructures, key services and primary transportation routes. The pedestrian and vehicular accessibility to these destination points within the road network is considered for the transport network analysis.

3 | Results

3.1 | Flood Model Validation

To support the validation of the flood model used, a comparison of reported and simulated flooding based on historical rain events is performed. These include the rain events of May 2011 and May 2013 (Oriental Bay), April and May 2015 (Southern CBD), January 2002 and May 2013 (Northern CBD). The reported flooding data used for model validation was derived from internally shared technical reports. A binary classification method for flood prediction is used to classify the flooded and non-flooded locations. Of the 88 reported flooding incidents, 85 of which were successfully predicted by the PCSWMM model, resulting in a prediction accuracy of approximately 93.2%. A sample comparison of the simulated and reported flooding in the study area is shown in Figure 6.

The alignment between the observed and predicted flooding indicates the effectiveness of applying the model in representing flood scenarios to be used for the transport network analysis.

3.2 | Risk for Pedestrians and Vehicles

The pedestrian and vehicle high-risk area maps, generated based on depth-only and depth-velocity stability thresholds during the rainfall peak ($t = 16$ h), are shown in Figures 7 and 8. The lighter yellow and red grids represent risks based solely on depth and integrated depth-velocity components, using the lower threshold pedestrian and vehicle stability risks. In contrast, the darker yellow and red grids represent risks based on upper thresholds.

At the maximum peak, the pedestrian risk areas for depth-only and depth-velocity thresholds are 0.06–0.15 and 0.11–0.51 km^2, respectively. While the vehicle risk areas for depth-only and depth-velocity thresholds are 0.11–0.22 and 0.13–0.30 km^2, respectively. The inclusion of the velocity threshold in the simulations results in an increase in pedestrian high- and medium-risk areas of 83.3% and 240.0%, while the high- and medium-risk areas for vehicles are calculated to be 18.2% and 36.4%, respectively. Flood velocity leads to higher risk for pedestrians, with an additional 0.05–0.36 km^2 area considered unsafe to navigate by foot, compared to 0.02–0.08 km^2 considered impassable for vehicles. This difference is highlighted by the greater number of depth-velocity grids shown in Figures 7 and 8 for pedestrians compared to vehicles for both high and medium risks.

To illustrate the number of road blockages in the study domain as the rainfall event progresses, the medium and high-risk depth-only (MRDO and HRDO) and depth-velocity (HRDO and HRDV) for pedestrians and vehicles are presented in Figure 9. The graph defines the time-increment changes in the number of road segments blocked during the event.

Across all risk assessments, the highest number of road closures is observed during the rainfall peak. When considering only depth-based risks, the percentage of impassable road segments ranges from 0.0% to 0.004% for pedestrians, and from 0.01% to 0.06% for vehicles. However, incorporating the velocity risks, the percentage of road segments deemed unsafe increases significantly, rising to 0.005%–0.08% for pedestrians and 0.07%–0.10% for vehicles, respectively.

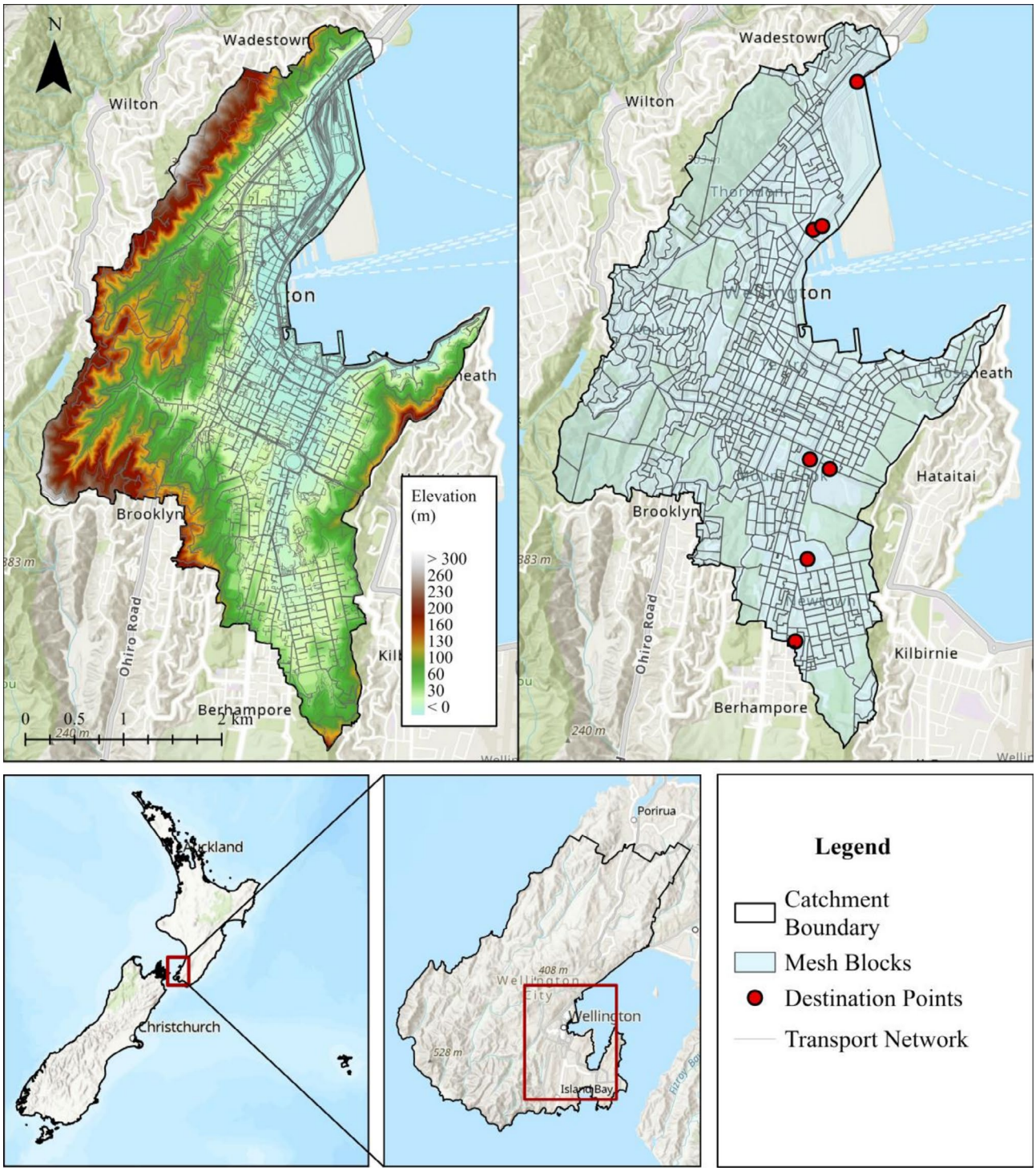

FIGURE 5 | Wellington city with the study sub-catchments Oriental Bay, Northern and Southern Central Business District, the meshblocks, the destination points and the transport network.

3.3 | Transport Network Accessibility

To determine the effect of the flood risk on the accessibility of the population to key destination zones, pedestrian and vehicle transport network analyses are performed considering dry conditions and incorporating the depth-only and depth-velocity risk obstructions in the transport network. Using the inbuilt route-finding algorithm within SUMO, the shortest route from each meshblock to the key locations is determined. For the analysis, a binary closure assumption is implemented, considering a road or multilane road segment as passable if depth-velocity values do not exceed the stability threshold, and impassable when the threshold is exceeded. This approach ensures that partial closures do not lead to an underestimation of the actual surrounding flow conditions, as illustrated in Figure 10. In a scenario where partial closures are applied, the areas surrounding a high-risk zone may still be classified as medium risk, potentially providing vehicle users with a false sense of assurance when traversing this particular road segment.

FIGURE 6 | Simulated and reported flooding in an intersection in Mount Cook, Wellington. Flood Image *Source:* Talk Wellington 2025; Stuff NZ 2025.

For this study, destination points are assigned for critical care facilities (Wellington Regional and Wakefield Hospitals), public transport services (Wellington Railway Station, Wellington Intercity Bus Terminal and Mount Victoria tunnel access to the airport) and bottleneck areas (Wellington Basin Reserve) (See Figure 5). The percentage of meshblocks and corresponding population with limited access to the assigned locations is summarised in Table 3.

When flood depth-based obstructions are applied to the transport network, approximately 0.3%–2.9% of the Wellington CBD population would be unable to access certain key locations on foot, while 1.3%–4.3% would be unable to do so by vehicle. On the other hand, the flood depth-velocity–based network analysis identified an increase in high-risk areas, which results in 2.3% of the population losing access on foot and 2.0% by vehicle, respectively. Furthermore, medium-risk areas identified in

FIGURE 7 | Pedestrian high and medium depth-only and depth-velocity risk maps at rainfall peak time (16 h).

the analysis would lead to an increase in the population without access up to 98.8% for pedestrians and 46.4% for vehicles, respectively.

The results show that a significant portion of the service population is identified to be potentially unable to access essential service areas when the depth-velocity risk is applied to the transport network. The steep characteristics of the area contributed to the high-velocity, relatively shallow flood flows. Due to the 'bottleneck' characteristics of the transport network in this area, even minimal obstructions could result in a large number of meshblock zones without possible access to the designated service areas. In addition, despite the flatter slopes towards the downstream flow direction, the density of buildings within this zone contributed to the channelization of flow onto the road network. However, the majority of the buildings within this area are large multi-storey offices and apartment complexes, which are unlikely to be directly at risk of low-level floods. It is recommended that travel be avoided in this area during the flood peak, with vertical relocation being a more appropriate strategy, especially considering the additional risks associated with carrying out such large-scale ground-level mobility in the transport network.

In addition to identifying meshblocks with restricted access to key services, the alternative path-finding algorithm generated alternative routes in the transport network for each meshblock.

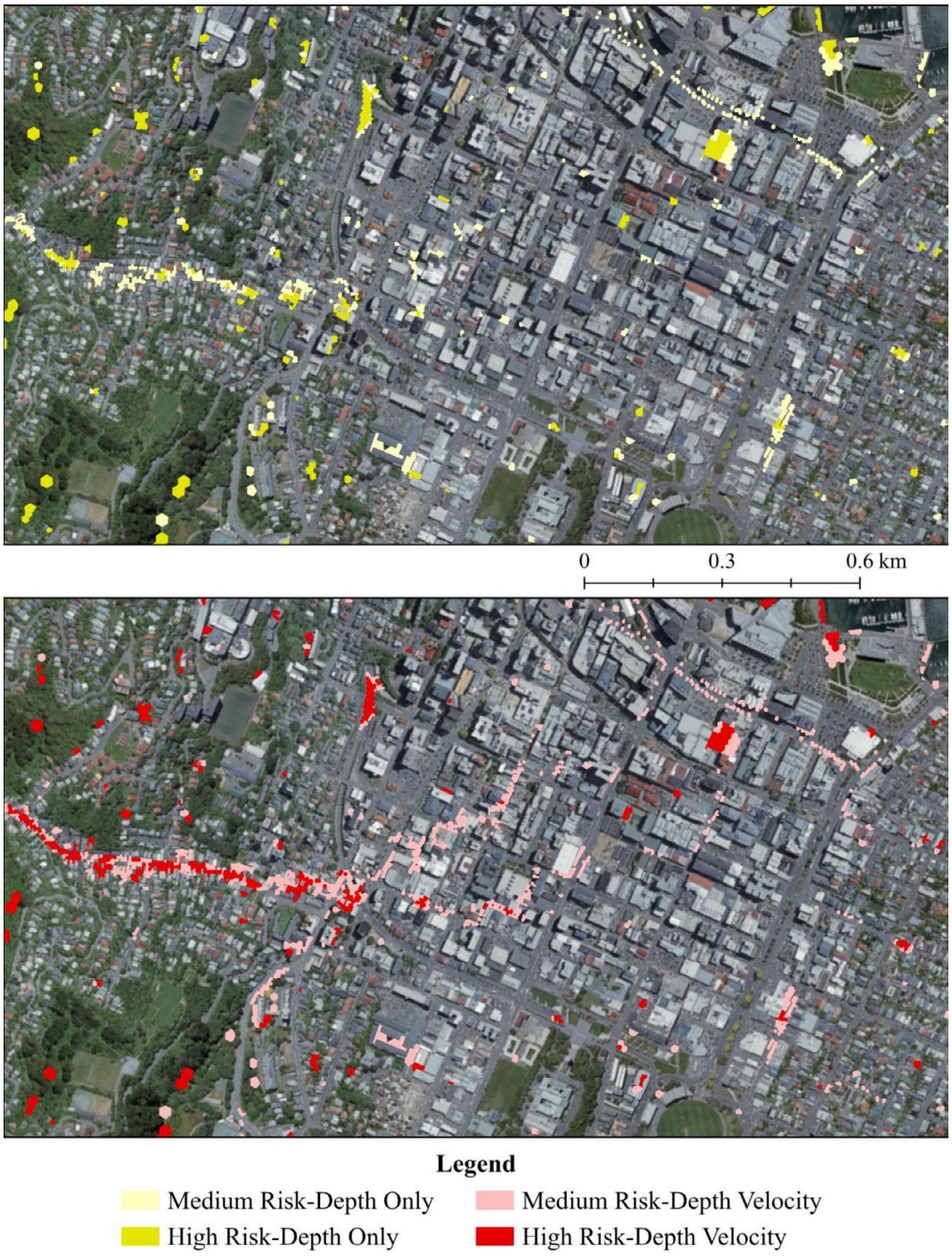

FIGURE 8 | Vehicle high and medium depth-only and depth-velocity risk maps at rainfall peak time (16 h).

The difference in travel distance during dry conditions when depth-only and depth-velocity are applied to the transport network for pedestrians and vehicles is shown in Figures 11 and 12, respectively.

The points closer to the diagonal line indicate the closeness of the travel distance during flood conditions and dry conditions. For the vehicle and pedestrian travel distance analysis, the majority of the travel distance for flooded conditions is longer than that of dry conditions, illustrated by the majority of points positioned above the diagonal line. The number of restricted and rerouted transport routes from individual meshblocks to service facilities is most pronounced under DV conditions. For vehicles, the percentage of meshblocks with no accessible routes increased from 1.6% to 4.9% under DO conditions to 2.0%–36.4% under DV conditions. For pedestrians, this increases from 0.0% (DO conditions) to 1.6%–4.9% (DV conditions). The percentage of rerouted transport access for vehicles is 37.7%–76.1% under DO and 38.3%–75.4% under DV conditions. For pedestrian access, these values increase from 0.0% to 40.5%–82.2% for DO and DV conditions, respectively. During MRDV conditions, the majority of the meshblock zones are found to have no access to destination zones, particularly Basin Reserve, Victoria Tunnel and Wakefield and Wellington Hospital when travelling on foot. For both pedestrian and vehicle reroute analysis,

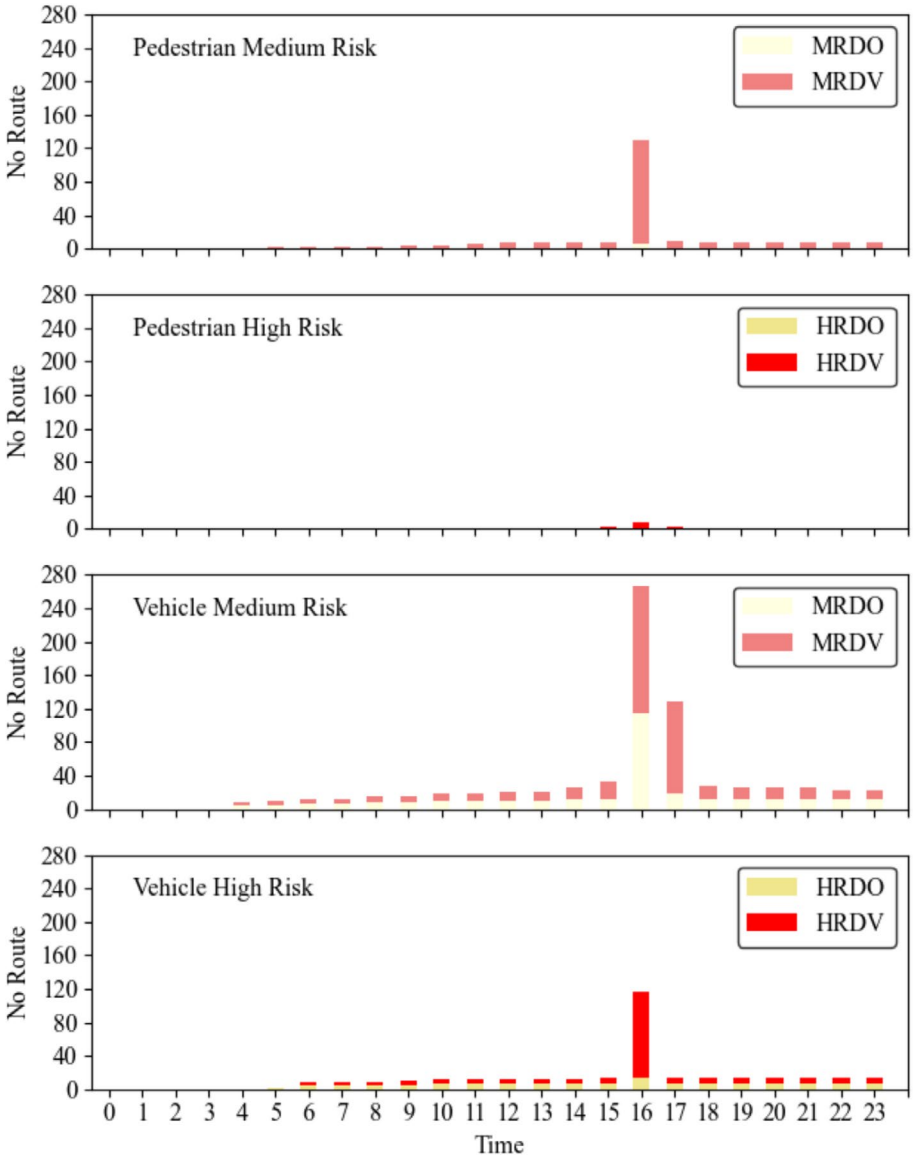

FIGURE 9 | Pedestrian and vehicle depth-only and depth-velocity risk no route comparison showing both for medium and high risk based on the 24 h storm event.

alternative routes are found, albeit generally having greater travel distance than that of dry conditions. Based on the vehicle accessibility analysis (Figure 12), MRDV conditions were also found to generate alternative routes with relatively longer travel distances compared to dry conditions, as indicated by the majority of points positioned farther from the diagonal reference line. In some cases, the reroute travel distance was shorter than the optimum route (as illustrated by the points located underneath the diagonal line in Figure 12), this outcome is attributed to SUMO's implementation of Dijkstra's algorithm which determines the shortest path based on travel time derived from road speed limits rather than physical distance.

4 | Discussion

The results show that flood risk mapping from a depth-only perspective could significantly underestimate the risks posed to pedestrians and vehicles when compared to depth-velocity based risk mapping. For the parameters modelled in this study, the high-risk areas from depth-only analyses were shown to have an underestimation of 18.2% for vehicles and 83.3% for pedestrians, while medium-risk areas are underestimated by 36.4% (vehicles) and 240.0% (pedestrians), respectively. For the study domain, depth-based risk analysis estimates that about 0.3%–2.9% (transiting on foot) and 1.3%–4.9% (transiting by vehicle) of the population have restricted access to certain key locations. When DV conditions are applied, these values can range from 2.2% (considering pedestrian high risk areas) and 2.0% (vehicle high risk areas) to 98.8% (pedestrian medium-risk areas) and 49.2% (vehicle medium-risk areas), respectively.

The results indicate a significant increase in the proportion of the transport network that becomes unsuitable for transit by pedestrians and vehicles when the flood flow velocity is included in the risk assessment. This discrepancy is more pronounced

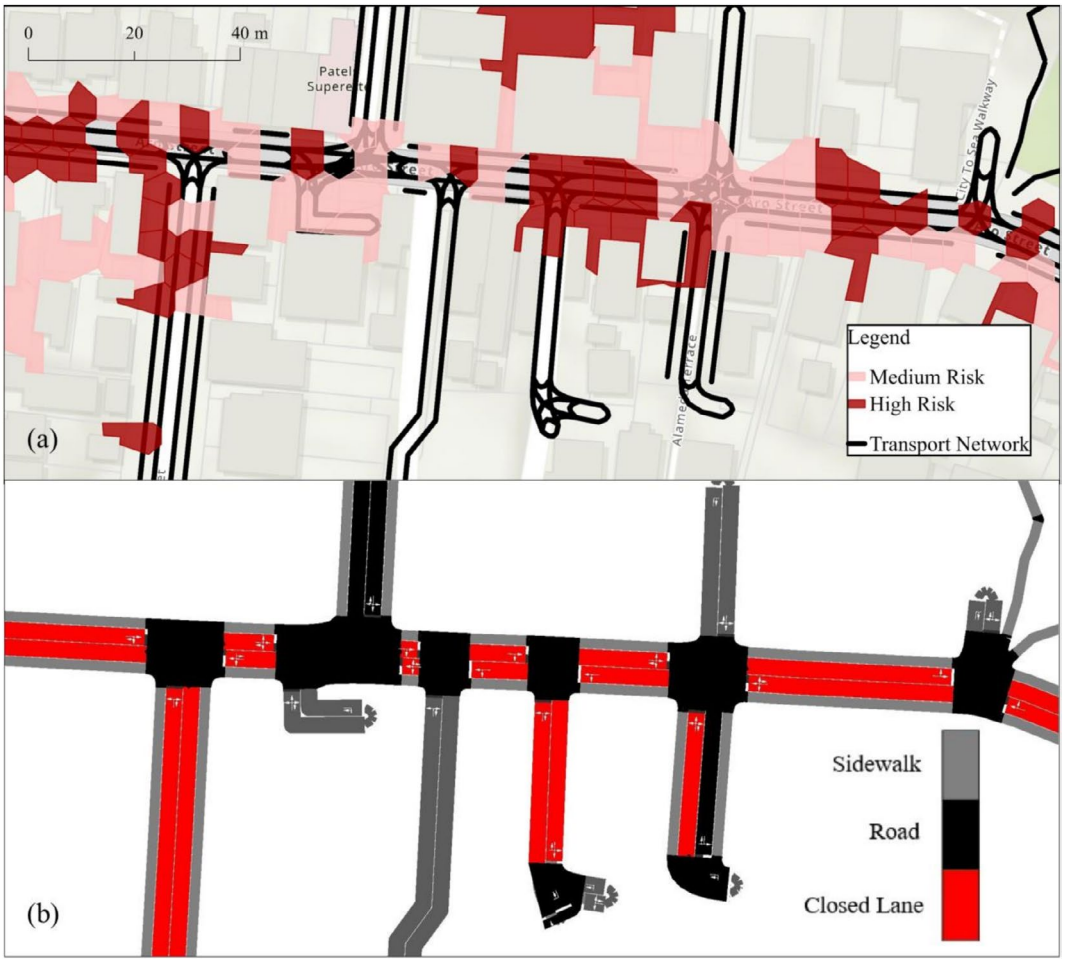

FIGURE 10 | Visualisation of (a) flood risk in the transport network and (b) corresponding closed lanes in SUMO without blanket closure.

TABLE 3 | Percentage (%) of meshblock zones and population without access to specified destination points based on the risk conditions.

		Destination zones						
Transport mode	**Conditions**	**Basin reserve**	**Victoria tunnel**	**Wakefield hospital**	**Wellington bus terminal**	**Wellington regional hospital**	**Wellington railway station**	**Affected population (%)**
Pedestrian	Dry	0.0	0.0	0.0	0.0	0.0	0.0	0.0
	MRDO	2.7	2.7	2.7	2.7	2.7	2.7	2.9
	HRDO	0.3	0.3	0.3	0.3	0.3	0.3	0.3
	MRDV	95.7	98.4	71.8	61.1	95.1	61.1	98.8
	HRDV	2.3	2.3	2.3	2.3	2.3	2.3	2.2
Vehicle	Dry	0.0	0.0	0.0	0.0	0.0	0.0	0.0
	MRDO	4.9	4.9	4.9	4.9	4.9	4.9	4.2
	HRDO	1.6	1.6	1.6	1.6	1.6	1.6	1.3
	MRDV	49.2	49.2	49.1	9.3	49.1	9.3	46.4
	HRDV	2.0	2.0	2.0	2.0	2.0	2.0	2.0

for steep terrain with high-density building settlements that are only accessible by constricted transport networks. Further to this, the results highlight the dynamic nature of risk during the event, emphasising the potential dangers posed to individuals attempting to traverse the transport network during the peak of the modelled event.

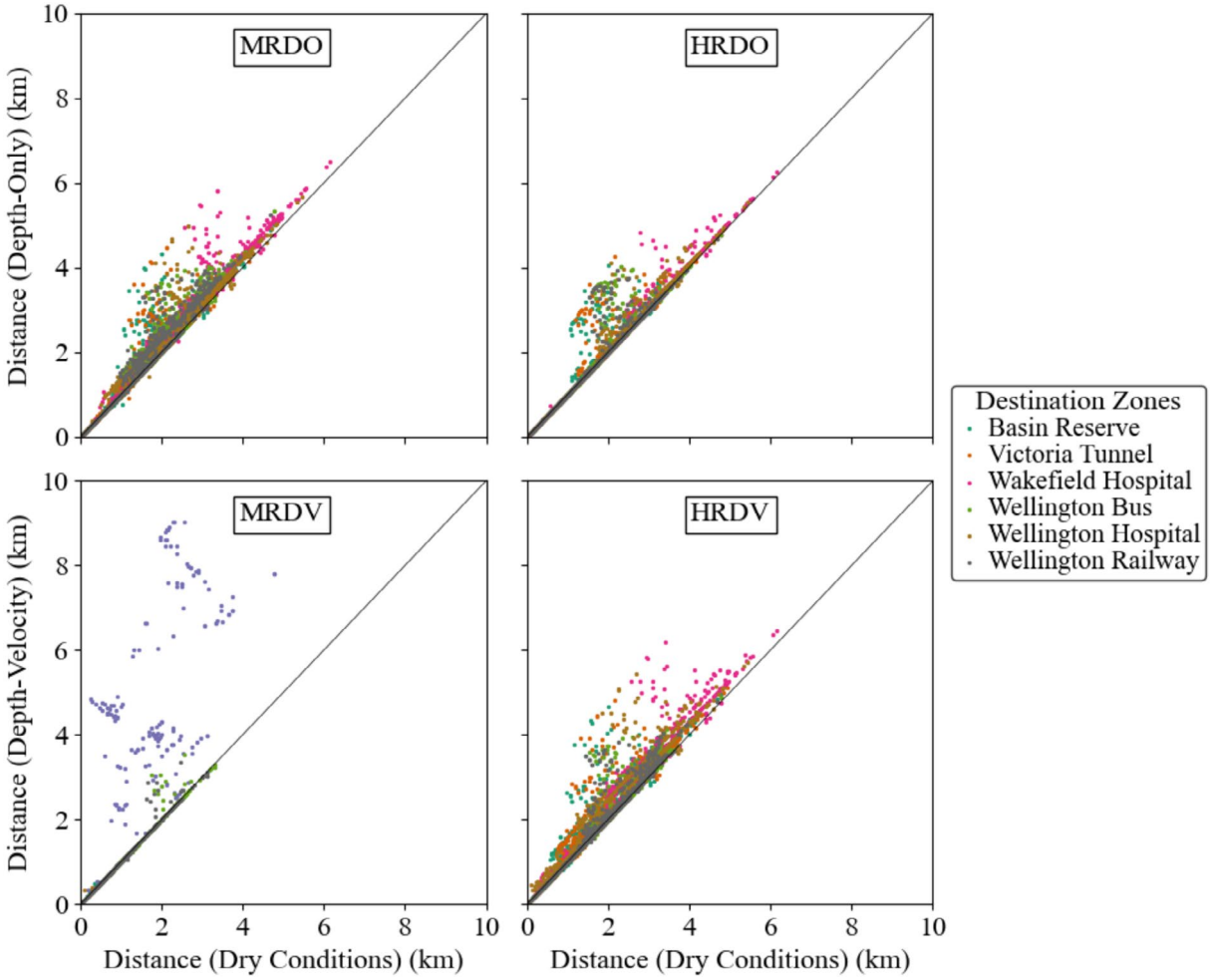

FIGURE 11 | Comparison of pedestrian travel distance under dry conditions, depth-only and depth-velocity re-routing conditions.

According to Hamilton et al. (2018), shallow flood water is often perceived to be safer to navigate than it is. Hence, it is crucial to identify flood-velocity prone areas, in addition to flood depth-prone areas, to mitigate these misconceptions. The network restrictions identified in the current work have varied impacts on the transport network. With risk predictions focused solely on flood depth, transport planning may inaccurately assess transport-safe areas, thereby exposing the transport users to heightened risk and further imposing complications on the transportation process. Following the framework introduced here, warnings based on flood depth-velocity risk mapping for pedestrians and vehicles can be issued using forecasted rainfall duration and intensity, enabling timely and informed decision-making for the urban population prior to the flood obstructions in the network system.

Several advantages of incorporating depth-velocity thresholds in the flood simulations were highlighted in the current work. However, the following limitations must be noted. Firstly, the study focused solely on pluvial flooding and did not incorporate the potential impacts imposed by river overflow, coastal tide fluctuations and the associated storm surge. Similarly, the exclusion of the infiltration process in the simulations may not be able to adequately represent short-duration flood events in the developed methodology. To better predict the flooding in different scenarios, the inclusion of the infiltration process, especially under dry initial conditions, could provide a more comprehensive understanding of its influence in urban flood dynamics. Furthermore, the analysis did not account for other potential rainfall-induced hazards, such as soil erosion and landslides. In urban catchments surrounded by mountainous areas, such as the study domain, road obstructions caused by landslides can pose a significant risk to the public. Given the potential risk, a comprehensive multi-hazard assessment is recommended to fully understand the risks associated with extreme weather events.

In addition, recent studies have indicated that the efficacy of public responses can be enhanced by understanding key factors of human behaviour that influence the evacuation decision-making process (McCaffrey et al. 2017). During extreme scenarios where evacuation is required, public response can be classified into these behavioural categories: individuals who are likely to evacuate immediately, those that are likely to wait and evaluate the situation before taking action, and those who choose to remain and defend. In this study, assumptions are made that the population maintains mobility, continuing to utilise the transport network during the event. In addition, a limitation of the approach outlined in this paper is the simplified depiction of movements, restricting agent pathways to linear segments within the network (e.g., sidewalks and roads).

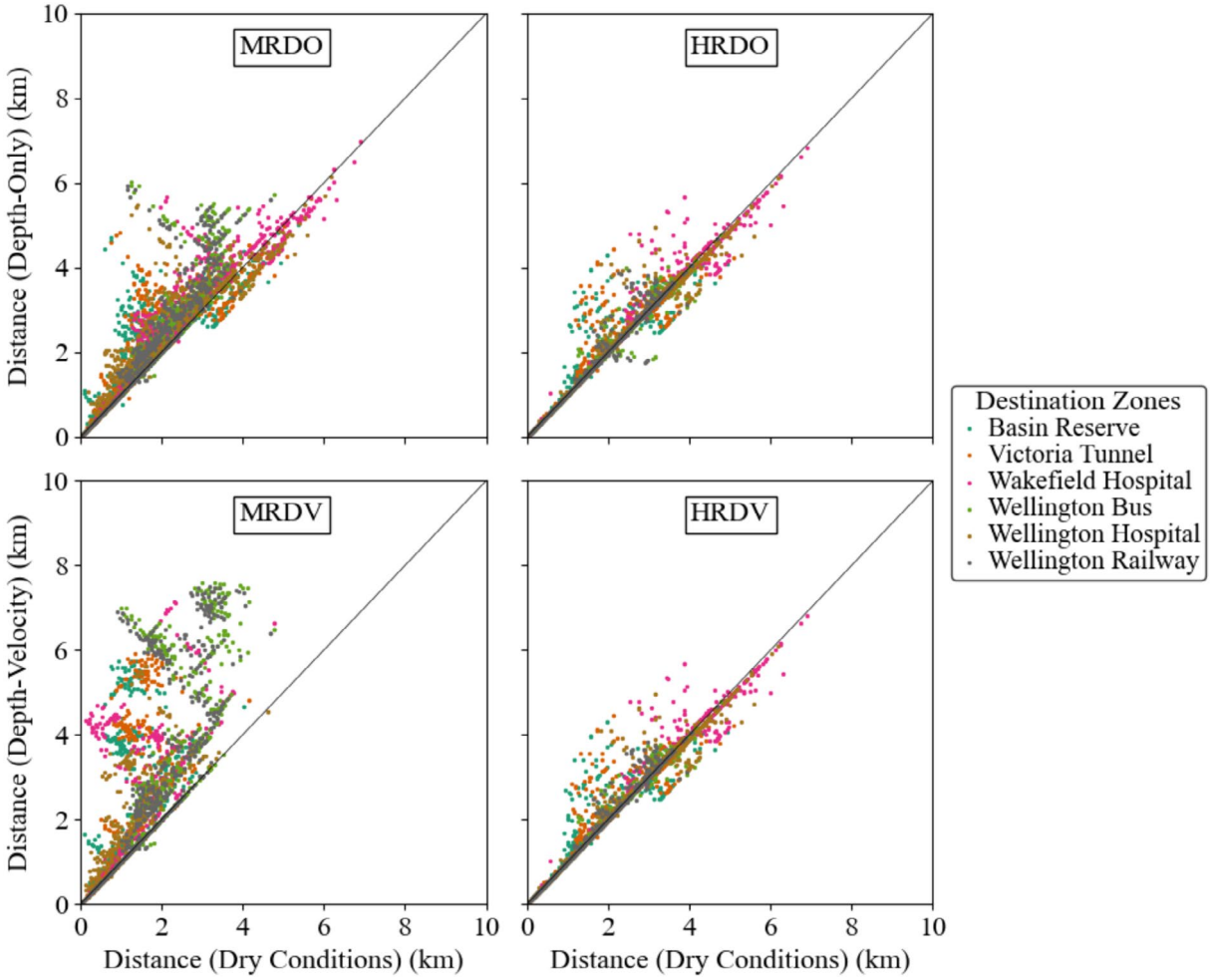

FIGURE 12 | Comparison of vehicle travel distance on dry conditions, depth-only and depth-velocity re-routing conditions.

Consequently, if a sidewalk is designated as obstructed by floodwater, the model does not account for real-world detours that agents might take, such as navigating along a grass verge or cutting across open fields. Therefore, whilst the model provides insights into regional accessibility reduction, the linear constraints may lead to an overestimation of inaccessible areas. The impact of the volume of people on the traffic system, the time of the day when evacuation occurs (whether people are at work, at home or elsewhere), the impact of a partial blockage, redirecting flow, optimising arrival time and the effect of considering only the percentage of early evacuees and wait-and-assess evacuees are the focus of future research.

Differences in transport mobility and accessibility to key locations across various scenarios investigated suggest that transport to certain zones can pose risks to pedestrians and vehicles when flow velocity risks are not properly accounted for. In some cases, possibilities of a population that has restricted access to these locations are found; additionally, alternative routes are computed for the public to use. The potential risks identified through the depth-stability functions in this study emphasises the importance of incorporating the flow velocity information, alongside flood depth, in transport mobility planning and management.

5 | Conclusions

This study presents an integrated framework for identifying flood risk areas that include both the depth and velocity components of a flood using a combined process of urban flood modelling, stability threshold and transport network analysis.

The findings suggest that conventional transport risk analysis methods, relying solely on flood depth, may underrepresent the risks to pedestrians and vehicle occupants during flood event evacuations. The risk significantly increases when the depth–velocity criterion is considered, particularly in steep, impervious catchments where the flow velocities of surface runoffs are exacerbated. A significant percentage of the population is found to have limited access to certain service areas during the rainfall peak, which may potentially increase the exposure of transport to risk and present challenges to ensure public safety during travel efforts. The inclusion of depth–velocity thresholds in flood risk mapping could introduce more effective emergency disaster planning, where travelling to emergency facilities and transport services could be planned in advance, reducing and mitigating potential risk in the events of extreme flooding. The results of this research can be used to analyse changes in the extent and distribution of risk in the road network throughout the duration

of the flood events. These insights enable effective early warning and guidance to the public before road closures, preventing simultaneous traffic mobility, reducing the risk of traffic congestion, and providing recommendations for alternative routes.

The combination of the depth-velocity stability function, 1D–2D hydraulic modelling and transport network analysis introduced in this study offers a valuable framework for enhancing disaster preparedness and transport mobility planning for urban areas facing future climate-induced flood events. This innovative management approach has the potential to significantly minimise the potential injuries and casualties and strengthen the resilience of the urban population to extreme events, while providing critical information to disaster decision makers in developing more adaptive policies and infrastructures, enabling cities to effectively prepare for the future challenges posed by the changing climate.

Acknowledgements

Lea Dasallas, Barry Evans, Markus Pahlow and Thomas A. Cochrane acknowledge funding from the European Union's Horizon Europe Framework Programme for Innovation 'Mitigating environmental disruptive events using people-centric predictive digital technologies to improve disaster and climate resilience' (Minority Report), Grant 101147385. The authors also acknowledge the Wellington City Council for providing access to data critical for the implementation of the research project.

Data Availability Statement

The data that support the findings of this study are available from the corresponding author upon reasonable request.

References

Adeke, D., and S. Mugume. 2025. "A Methodology for Development of Flood-Depth-Velocity Damage Functions for Improved Estimation of Pluvial Flood Risk in Cities." *Journal of Hydrology* 653: 132736.

Ahiablame, L., and R. Shakya. 2016. "Modeling Flood Reduction Effects of Low Impact Development at a Watershed Scale." *Journal of Environmental Management* 171: 81–91.

Bertsch, R., V. Glenis, and C. Kilsby. 2017. "Urban Flood Simulation Using Synthetic Storm Drain Networks." *Water* 9, no. 12: 925.

Bibi, T. S., K. G. Kara, H. J. Bedada, and R. D. Bededa. 2023. "Application of PCSWMM for Assessing the Impacts of Urbanization and Climate Changes on the Efficiency of Stormwater Drainage Systems in Managing Urban Flooding in Robe Town, Ethiopia." *Journal of Hydrology: Regional Studies* 45: 101291.

Bisht, D. S., C. Chatterjee, S. Kalakoti, P. Upadhyay, M. Sahoo, and A. Panda. 2016. "Modeling URBAN Floods and Drainage Using SWMM and MIKE URBAN: A Case Study." *Natural Hazards* 84: 749–776.

Bronstert, A., D. Niehoff, and G. R. Schiffler. 2022. "Modelling Infiltration and Infiltration Excess: The Importance of Fast and Local Processes." *Hydrological Processes* 37: 1–20.

Chowdhury, M., and T. Chakraborty. 2024. "Calibration of SUMO Microscopic Simulation for Heterogeneous Traffic Condition: The Case of the City of Khulna, Bangladesh." *Transportation Engineering* 18: 100281.

Computational Hydraulics Inc. 2025. "PCSWMM: Advanced Modeling Software for Stormwater, Wastewater, Watershed and Water Distribution Systems." Accessed November 4, 2025. https://www.pcswmm.com/.

Cox, R. J., T. D. Shand, and M. J. Blacka. 2011. "Australian Rainfall and Runoff: Appropriate Safety Criteria for People." Engineers Australia. https://arr.ga.gov.au/arr-guideline/revision-projects/project-list/projects/project-10.

de Castro-Ferreira, E., A. C. da Silva, P.-C. J. J. Cabral, and J. R. Azevedo. 2022. "Evaluation of Hydrological Parameters of the Goiana River Basin in the State of Pernambuco Using the Automatic Calibration Tool of the Hydrodynamic Model PCSWMM in Multiple Fluviometric Stations." *Research, Society and Development* 12: e15011225331.

Du, B., M. Wang, J. Zhang, Y. Chen, and T. Wang. 2025. "Urban Flood Prediction Based on PCSWMM and Stacking Integrated Learning Model." *Natural Hazards* 121: 1971–1995.

Eclipse SUMO. 2025. "Simulation of Urban MObility." https://eclipse.dev/sumo/.

Environmental Protection Agency. 2015. "Storm Water Management Model User Manual Version 5.1." US EPA. EPA-600/R-14/413b.

Evans, B., A. Chen, S. Djordjević, J. Webber, A. Gómez, and J. Stevens. 2020. "Investigating the Effects of Pluvial Flooding and Climate Change on Traffic Flows in Barcelona and Bristol." *Sustainability* 12, no. 6: 2330.

Evans, B., M. Lam, C. West, et al. 2023. "A Combined Stability Function to Quantify Flood Risks to Pedestrians and Vehicle Occupants." *Science of the Total Environment* 908: 168237.

Falconer, R., P. Guo, Q. Chen, S. Deng, and J. Xia. 2015. "Stability Criterion for People in Floods for Various Slopes." *Proceedings of the ICE—Water Management* 169: 1–10.

Fathianpour, A., B. Evans, M. B. Jelodar, and S. Wilkinson. 2023. "Tsunami Evacuation Modelling via Micro-Simulation Model." *Progress in Disaster Science* 17: 100277.

Filippidis, L., P. Lawrence, V. Pellacini, A. Veeraswamy, D. Blackshields, and E. R. Gale. 2020. "Multimodal Wildfire Evacuation at the Microscopic Level." In *SafeGreece 2020 On-Line Proceedings*, 193–196. SafeGreece.

Flores, V., F. O. de Sousa, and S. Oda. 2024. "Enhancing Risk Management in Road Infrastructure Facing Flash Floods through Epistemological Approaches." *Buildings* 14, no. 7: 1931. https://doi.org/10.3390/buildings14071931.

Haan, C. T., B. J. Barfield, and J. C. Hayes. 1994. "3 - Rainfall-Runoff Estimation in Storm Water Computations." *Design Hydrology and Sedimentology for Small Catchments*: 37–103. https://doi.org/10.1016/B978-0-08-057164-5.50007-4.

Hamilton, K., A. Peden, J. Keech, and M. Hagger. 2018. "Changing People's Attitudes and Beliefs Toward Driving Through Floodwaters: Evaluation of a Video Infographic." *Transportation Research Part F: Traffic Psychology and Behaviour* 53: 50–60.

Harris, D., R. Tuke, D. Smith, and M. Hughes. 2021. *Framework for Evacuation Routes*. Waka Kotahi NZ Transport Agency Research Report 681. 1–80.

He, K., M. Pregnolato, N. Carhart, J. Neal, and R. De Risi. 2024. "Functionality Assessment of Road Network Combining Flood Roadworthiness and Graph Topology." *Transportation Research Part D: Transport and Environment* 135: 104354.

Hettiarachchi, S., C. Wasko, and A. Sharma. 2018. "Increase in Flood Risk Resulting From Climate Change in a Developed Urban Watershed—The Role of Storm Temporal Patterns." *Hydrology and Earth System Sciences* 22: 2041–2056.

Hsu, M. H., S. H. Chen, and T. J. Chang. 2000. "Inundation Simulation for Urban Drainage Basin With Storm Sewer System." *Journal of Hydrology* 234: 21–37.

Ivanov, A., and F. Abu-Abed. 2019. "Usage of SUMO Computer Modeling Software for Road Traffic Control System Validation." *International Journal of Recent Technology and Engineering* 8, no. 2: 4662–4666.

Jeffers, S., and F. Montalto. 2018. "Modeling Urban Sewers With Artificial Fractal Geometries." *Journal of Water Management Modeling* 26: C455.

Land Information New Zealand. 2024. "LINZ Online Data Service." https://data.linz.govt.nz/.

Le, H. N., D.-P. Vo, Q. D. Nguyen, B. Q. Nguyen, and C. C. Nguyen. 2024. "Assessing the Impacts of Urbanization and Climate Change on Urban Drainage System." *River* 3: 181–190.

Lee, H. K., B. H. Son, Y. C. Kim, and W. H. Hong. 2024. "Evacuation Information Methodology That Combined a Flooded Environment and Pedestrian Behavioral Model." *International Journal of Disaster Risk Reduction* 106: 104438.

Lopez, P. A., M. Behrisch, L. Bieker-Walz, et al. 2018. "Microscopic Traffic Simulation Using SUMO." In *IEEE Intelligent Transportation Systems Conference (ITSC)*, 2575–2582. IEEE.

Ma, X., X. Hu, T. Weber, and D. Schramm. 2021. "Evaluation of Accuracy of Traffic Flow Generation in SUMO." *Applied Sciences* 11, no. 6: 2584.

Manchikatla, S., and N. Umamahesh. 2022. "Simulation of Flood Hazard, Prioritization of Critical Sub-Catchments, and Resilience Study in an Urban Setting Using PCSWMM: A Case Study." *Water Policy* 24, no. 8: 1247.

Martínez-Gomariz, E., M. Gómez, and B. Russo. 2016. "Experimental Study of the Stability of Pedestrians Exposed to Urban Pluvial Flooding." *Natural Hazards* 82: 1259–1278.

Martínez-Gomariz, E., M. Gómez, B. Russo, and S. Djordjevic. 2017. "A New Experiments-Based Methodology to Define the Stability Threshold for Any Vehicle Exposed to Flooding." *Urban Water Journal* 14, no. 19: 930–939.

McCaffrey, S., S. Wilson, and A. Konar. 2017. "Should I Stay or Should I Go Now? Or Should I Wait and See? Influences on Wildfire Evacuation Decisions." *Risk Analysis* 38, no. 7: 1390–1404.

Melo, N., B. F. Santos, and J. Leandro. 2014. "A Prototype Tool for Dynamic Pluvial-Flood Emergency Planning." *Urban Water Journal* 12, no. 1: 79–88.

National Institute of Water and Atmospheric Research. 2018. "High Intensity Rainfall Design Version 4." Envirolink.

National Institute of Water and Atmospheric Research. 2024a. "Extreme Weather—Heavy Rainfall." National Institute of Water and Atmospheric Research. https://niwa.co.nz/hazards/extreme-weather-heavy-rainfall.

National Institute of Water and Atmospheric Research. 2024b. "High Intensity Rainfall Design System V4." https://hirds.niwa.co.nz/.

OpenStreetMap Contributors. 2025. "OpenStreetMap." https://www.openstreetmap.org.

Pants, R., S. Thacker, J. W. Hall, D. Alderson, and S. Barr. 2018. "Critical Infrastructure Impact Assessment due to Flood Exposure." *Journal of Flood Risk Management* 11: 22–23.

Paquier, A., E. Mignot, and P. Bazin. 2015. "From Hydraulic Modelling to Urban Flood Risk." *Procedia Engineering* 115: 37–44.

Petrucci, O., T. Caloiero, A. Pasqua, P. Perrotta, L. Russo, and C. Tansi. 2017. "Civil Protection and Damaging Hydrogeological Events: Comparative Analysis of the 2000 and 2015 Events in Calabria." *Advances in Geosciences* 44: 101–113.

Pregnolato, M., A. Ford, S. M. Wilkinson, and R. J. Dawson. 2017. "The Impact of Flooding on Road Transport: A Depth-Disruption Function." *Transportation Research Part D: Transport and Environment* 55: 67–81.

Rahman, R., S. Hasan, and M. Zaki. 2019. "Towards Reducing the Number of Crashes During Hurricane Evacuation: Assessing the Potential Safety Impact of Adaptive Cruise Control Systems." *Transportation Research Part C: Emerging Technologies* 128: 103188.

Randall, M., N. Perera, N. Gupta, and M. Ahmad. 2017. "Development and Calibration of Dual Drainage Model for the Cooksville Creek Watershed, Canada." *Journal of Water Management Modeling* 25: C419.

Sangal, S., and S. R. Bonema. 1994. "A Methodology for Calibrating SWMM Models." *Journal of Water Management Modeling* 1001: R176-24.

Sidek, L., L. Chua, A. Azizi, H. Basri, A. Jaafar, and W. Moon. 2021. "Application of PCSWMM for the 1-D and 1-D–2-D Modelling of Urban Flooding in Damansara Catchment, Malaysia." *Applied Sciences* 11, no. 1: 9300.

Stats New Zealand. 2024. "2018 Census Electoral Population (Meshblock 2020)." https://datafinder.stats.govt.nz/layer/104578-2018-census-electoral-population-meshblock-2020/.

Stuff NZ. 2025. "Wellington Left Mopping Up Flooded Homes Again." https://www.stuff.co.nz/national/68485217/wellington-left-mopping-up-flooded-homes-again.

Talk Wellington. 2025. "Wet Wet Wellington." https://talkwellington.org.nz/2018/wet-wet-wetlington/.

Wellington City Council. 2024. "WCC ArcGIS REST Services Directory." https://services7.arcgis.com/2ECs938g489DMWjt/ArcGIS/rest/services.

Wellington Water. 2019. "Reference Guide for Design Storm Hydrology." In *Wellington Water, Wellington*. Wellington Water. https://www.wellingtonwater.co.nz/assets/Resources/Developing/Reference-Guide-for-Design-Storm-Hydrology-April-2019.pdf.

Wellington Water. 2021. *Regional Standard for Water Services*. Wellington Water. https://www.wellingtonwater.co.nz/assets/Reports-and-Publications/Regional-Standard-RSWS.pdf.

Yang, Y., J. Yin, D. Wang, et al. 2023. "ABM-Based Emergency Evacuation Modelling During Urban Pluvial Floods: A Pluvial Flood Event Study in Zhengzhou, Henan Province." *Science China: Earth Sciences* 66: 282–291.

Zhang, Z., and C. Valeo. 2022. "Verification of PCSWMM'S LID Processes and Their Scalability Over Time and Space." *Frontiers in Water* 4: 1–23.